

more than $10^5 \Omega^{-1} \text{cm}^{-1}$, an estimate limited by contact effects and most likely carried by inhomogeneous filamentary conduction. We attribute this phenomenon to the crossover to a regime of free sliding CDW first proposed by Fröhlich as CDW superconductivity (24). Such a crossover has been observed in conventional CDWs, and is expected to occur once the density wave reaches velocities at which the background quasi-particles can no longer screen the response (25). An upper limit of the field at this second threshold may be estimated from the average pinning frequency $E_T^{(2)} \leq (\Omega_D^2/\Omega_p^2)(\rho_c/Q)$, where ρ_c is the collective charge density and $2\pi/Q$ is the period of the density wave. Assuming $2e$ per ladder (where e is electronic charge) contributing to the density wave, we obtain $E_T^{(2)} \leq 100 \text{ V/cm}$, again consistent with our measurements. Note that the true threshold for deformable sliding of the density wave is always much lower.

Now we turn to high-temperature Raman measurements. The Raman response function is proportional to $\Im\epsilon_L$. The comparison of the Raman and ac transport data is not straightforward because only above room temperature is $\Gamma(T)$ large enough for a Raman QEP to be observed. Although $\Gamma(T)$ extracted from the Raman data exhibits activated behavior with a gap consistent with dc conductivity above T^* , the values for $\Gamma(T)$ are about 50 times the relaxational energies predicted from Eq. 5. However, the lowering of the peak intensity with increasing temperature (see Fig. 2B, inset) suggests that there is a reduction of the density wave amplitude ρ_c , which would produce a concomitant increase in Γ . Further enhancement in the scattering rate may come from additional relaxation due to the presence of low-lying states seen at temperatures above T^* by magnetic resonance (9), high-frequency Raman scattering (26), and c -axis optical conductivity (22).

All our results have clear quantitative parallels with sliding density wave transport phenomena observed in established C/SDW materials, yet there must be a number of important microscopic differences from conventional weak-amplitude C/SDWs. The C/SDW correlation in $\text{Sr}_{14}\text{Cu}_{24}\text{O}_{41}$ is a high-temperature phenomenon that we observe (with diminishing amplitude) up to the highest measured temperature, 630 K. Such high-temperature correlations cannot be supported by phonons, which suggests that the charge-spin correlations arise from strong spin exchange interactions with characteristic energy scale $J \approx 1300 \text{ K}$ (26). The magnetic excitations in spin $1/2$ two-leg ladders are resonating valence bond (RVB) quantum states (1, 3, 26, 27), different from the gapless classical spin waves in the SDW systems. Theoretical calculations for a doped two-leg spin ladder suggest that in an RVB environment the holes are paired in a state of approximate d -wave symmetry with a few lattice spacings in size (28–30). The

superconducting condensation of bound pairs is competing with a crystalline order of these pairs in a CDW state (10). If the fundamental current-carrying object in the doped singlet ladders is a bound pair of holes, the hydrodynamic mode we have discussed involves local displacement of “crystallized” pairs, screened by charged excitations across the CDW gap, which would account for the appearance of the conductivity as the relevant parameter to describe backflow. Nevertheless, our observation of a weakly pinned mode—which implies a large stiffness for charged fluctuations of the order parameter—is surprising in the context of models with strong short-range correlations, where one would expect that lattice pinning effects are strong.

References and Notes

1. E. Dagotto, T. M. Rice, *Science* **271**, 618 (1996).
2. E. Dagotto, *Rep. Prog. Phys.* **62**, 1525 (1999) and references therein.
3. S. Sachdev, *Science* **288**, 475 (2000) and references therein.
4. E. M. McCarron III, M. A. Subramanian, J. C. Calabrese, R. L. Harlow, *Mater. Res. Bull.* **23**, 1355 (1988).
5. T. Siegrist, L. F. Schneemeyer, S. A. Sunshine, J. V. Waszczak, R. S. Roth, *Mater. Res. Bull.* **23**, 1429 (1988).
6. T. Osafune, N. Motoyama, H. Eisaki, S. Uchida, *Phys. Rev. Lett.* **78**, 1980 (1997).
7. M. W. McElfresh, J. M. D. Coey, P. Strobel, S. von Molnar, *Phys. Rev. B* **40**, 825 (1989).
8. H. Kitano *et al.*, *Europhys. Lett.* **56**, 434 (2001).
9. M. Takigawa, N. Motoyama, H. Eisaki, S. Uchida, *Phys. Rev. B* **57**, 1124 (1998).

10. E. Dagotto, J. Riera, D. J. Scalapino, *Phys. Rev. B* **45**, 5744 (1992).
11. M. Uehara *et al.*, *J. Phys. Soc. Jpn.* **65**, 2764 (1996).
12. N. Motoyama, T. Osafune, T. Kakeshita, H. Eisaki, S. Uchida, *Phys. Rev. B* **55**, R3386 (1997).
13. A. Gozar *et al.*, <http://arXiv.org/abs/cond-mat/0207219> (2002).
14. S. Havriliak, S. Negami, *J. Polym. Sci. C* **14**, 99 (1966).
15. G. Grüner, L. C. Tippie, J. Sanny, W. G. Clark, N. P. Ong, *Phys. Rev. Lett.* **45**, 935 (1980).
16. W.-Y. Wu, L. Mihály, G. Mozurkewich, G. Grüner, *Phys. Rev. Lett.* **52**, 2382 (1984).
17. R. J. Cava *et al.*, *Phys. Rev. B* **30**, 3228 (1984).
18. R. J. Cava, P. Littlewood, R. M. Fleming, R. G. Dunn, E. A. Rietman, *Phys. Rev. B* **33**, 2439 (1986).
19. L. Degiorgi, B. Alavi, G. Mihály, G. Grüner, *Phys. Rev. B* **44**, 7808 (1991).
20. G. Grüner, *Density Waves in Solids* (Perseus, Cambridge, MA, 1994).
21. P. B. Littlewood, *Phys. Rev. B* **36**, 3108 (1987).
22. H. Eisaki *et al.*, *Physica C* **341–348**, 363 (2000).
23. A. Zettl, G. Grüner, A. H. Thompson, *Phys. Rev. B* **26**, 5760 (1982).
24. H. Fröhlich, *Proc. R. Soc. London Ser. A* **223**, 296 (1954).
25. P. B. Littlewood, *Solid State Commun.* **65**, 1347 (1988).
26. A. Gozar *et al.*, *Phys. Rev. Lett.* **87**, 197202 (2001).
27. P. W. Anderson, *Science* **235**, 1196 (1987).
28. M. Sigrist, T. M. Rice, F. C. Zhang, *Phys. Rev. B* **49**, 12058 (1994).
29. M. Troyer, H. Tsunetsugu, T. M. Rice, *Phys. Rev. B* **53**, 251 (1996).
30. S. R. White, D. J. Scalapino, *Phys. Rev. B* **55**, 6504 (1997).
31. We thank A. P. Ramirez for help with ac transport measurements and for discussions. Supported by a Grant-in-Aid for Scientific Research and a COE grant from the Ministry of Education, Japan (S.U.).

1 February 2002; accepted 31 May 2002

Delocalization of Protons in Liquid Water

H. J. Bakker* and H.-K. Nienhuys†

We find that the vibrational potential of the O-H stretch vibrations of liquid water shows extreme anharmonicity that arises from the O-H···O hydrogen bond interaction. We observe that already in the second excited state of the O-H stretch vibration, the hydrogen atom becomes delocalized between the oxygen atoms of two neighboring water molecules. The energy required for this delocalization is unexpectedly low and corresponds to less than 20% of the dissociation energy of the O-H bond of the water molecule in the gas phase.

Liquid water possesses many remarkable properties that to a large extent can be explained by its extremely high density of hydrogen bonds. One of these properties is the anomalously high mobility of protons and hydroxyl ions (OH^-) in this liquid. This phenomenon has been explained from a (Grotthuss) conduction mechanism (1) that involves the exchange of the chemical O-H

bond and the hydrogen bond in the O-H···O hydrogen-bonded system formed by an $\text{H}_3\text{O}^+/\text{OH}^-$ ion and an H_2O molecule (2–4).

Relatively little is known about the effects of hydrogen bond interactions in liquid water on the reactivity of the O-H groups of the water molecule. In most molecular dynamics simulations, these effects are not included. Even in the most advanced Car-Parrinello molecular dynamics simulations, these effects are not well accounted for because the nuclear coordinates are described classically. In view of the small mass of the hydrogen atom and the proton, such a classic approach gives a poor description of the properties of

FOM Institute for Atomic and Molecular Physics, Kruislaan 407, 1098 SJ Amsterdam, Netherlands.

*To whom correspondence should be addressed. E-mail: bakker@amolf.nl

†Present address: Department of Chemical Physics, Lund University, Box 124, 221 00 Lund, Sweden.

the O-H groups of the water molecule. The effects of hydrogen bonding on the O-H bonds of water can in principle be studied by a spectroscopic investigation of the different vibrational quantum states of the O-H stretch vibrations. Unfortunately, such a study is strongly complicated by the ultrafast (subpicosecond) energy equilibration of liquid water (5). Therefore, the experimental study of the excited vibrational states of the hydrogen-bonded O-H groups of the water molecule requires the use of ultrafast (i.e., femtosecond) mid-infrared (mid-IR) spectroscopy. This type of spectroscopy has recently been applied successfully to the study of the vibrational relaxation (6, 7), molecular reorientation (8), and hydrogen bond dynamics (9–11) of different isotopic varieties of liquid water.

We investigated the effect of the O-H...O hydrogen bond interaction and dynamics on the spectral response of the O-H stretch vibrations of liquid water. We used a solution of HDO in D₂O instead of pure H₂O, because the spectral dynamics of H₂O is strongly affected by Förster energy transfer (12). In general, one should be careful when using HDO:D₂O as a model for H₂O, because the properties of HDO:D₂O, such as its vibrational relaxation, can be very different. However, in this case HDO:D₂O forms a good model system for water, because the hydrogen bond interaction and dynamics are similar for the different isotopic varieties of water.

In the experiment, the O-H stretch vibration of ~3% of the HDO molecules is excited with an intense mid-IR pump pulse with a pulse duration of 200 fs (13). The transient spectral changes induced by this excitation are monitored with a second, independently tunable, mid-IR probe pulse. The pump and probe pulses are both tunable between 2.7 and 4 μm (2500 to 3700 cm⁻¹). In Fig. 1, transient absorption spectra of the O-H stretch vibration are presented that were measured at three different

delays after excitation with a pump pulse with a central frequency of 3420 cm⁻¹. The shape of these spectra is independent of the excitation density, i.e., the energy of the pump pulse. For probe frequencies >3280 cm⁻¹, the signal is positive and results from bleaching of the $\nu = 0 \rightarrow 1$ transition [$\ln(T/T_0) > 0$, where T is the transmission of the probe and T_0 the transmission of the probe in the absence of the pump]. For probe frequencies <3280 cm⁻¹, the signal is negative and results from the induced $\nu = 1 \rightarrow 2$ absorption [$\ln(T/T_0) < 0$]. It is not possible to measure the transient spectral response at frequencies <2800 cm⁻¹, because the D₂O solvent absorbs in this frequency region. The amplitude of the transient absorption spectra rapidly decreases with delay as a result of the fast vibrational relaxation. The relaxation eventually results in a heating of the sample by ~1 K. The effect of this heating is a small, long-lived decrease and blue shift of the O-H stretch absorption band, which can be observed at delays >3 ps. In Fig. 2, the probe transmission at different frequencies is presented as a function of delay. These measurements form cross-sections of the transient spectra shown in Fig. 1. At a frequency of 2840 cm⁻¹, the signal rises much more slowly than at the other frequencies and attains its minimum transmission only after 450 fs. This result shows that the induced $\nu = 1 \rightarrow 2$ absorption spectrum undergoes a marked redshift in the first 500 fs after excitation.

The bleaching part of the signal shown in Fig. 1 has the nearly symmetric Gaussian shape of the linear absorption spectrum of the O-H stretch vibration of HDO dissolved in D₂O (10, 11). In contrast, the spectral shape of the $\nu = 1 \rightarrow 2$ induced absorption is much broader and steeper on the high-frequency side than on the low-frequency side. The $\nu = 1 \rightarrow 2$ transition also shows a quite large anharmonic shift of ~300 cm⁻¹ with respect to the $\nu = 0 \rightarrow 1$ transition. For comparison, for free (not hydrogen-bonded) water molecules, this shift has been measured to be ~100 cm⁻¹ (14). The

strong differences between the spectra of the $\nu = 0 \rightarrow 1$ and the $\nu = 1 \rightarrow 2$ transitions show that the potential of the O-H stretch vibration of liquid water must be extremely anharmonic. This anharmonicity is surprising, because excitation of the $\nu = 2$ state requires an energy of ~6500 cm⁻¹, whereas the O-H bond has a dissociation energy in the gas phase of ~40,000 cm⁻¹.

The anharmonic interaction between the O-H stretch vibration and the hydrogen bond can be described with the Lippincott-Schroeder (LS) model (15). In this model, there is a potential-energy term that depends both on the length r of the O-H bond and the oxygen-oxygen distance R of the O-H...O hydrogen bond. This potential $V_1(r,R)$ is shown in Fig. 3. The total potential energy of the O-H...O system consists of the sum of $V_1(r,R)$ and a potential-energy term $V_{II}(R)$ that depends only on R and that expresses the electrostatic attraction of two water molecules at large distances and their repulsion at short distances. $V_{II}(R)$ determines to a large extent the distribution of oxygen-oxygen distances R of liquid water. For $V_{II}(R)$ we use a Morse potential [$V_{II}(R) = D_{II}(1 - e^{-m_1(R - R_0)})^2$, with $D_{II} = 2000$ cm⁻¹, $n_{II} = 2.9 \times 10^{10}$ m⁻¹, and $R_0 = 2.88 \times 10^{-10}$ m]. With this potential, the distribution of R has the correct mean value of 2.85×10^{-10} m and width of 0.36×10^{-10} m (full-width at half-maximum) at 298 K, and the hydrogen bond has the correct dissociation energy (~2000 cm⁻¹) and stretch frequency (~200 cm⁻¹) (16).

In the past, the LS model was used classically, and the O-H stretch frequency was determined from a harmonic approximation. Here we use the potential $V_1(r,R)$ in a quantum-mechanical calculation of the vibrational wave functions and eigenenergies of the O-H

Fig. 1. Transient spectra of 0.5 M HDO dissolved in liquid D₂O at three different delays. The solid curves represent transient spectra calculated with the quantum-mechanical LS model. The strong broadening of the $\nu = 1 \rightarrow 2$ spectrum to lower frequencies results from the delocalization of the proton between the two oxygen atoms of the O-H...O system in the $\nu = 2$ state. The dashed curve represents the experimental $\nu = 0 \rightarrow 1$ absorption spectrum.

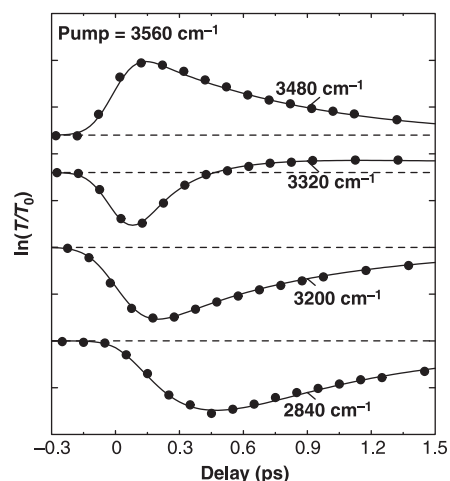
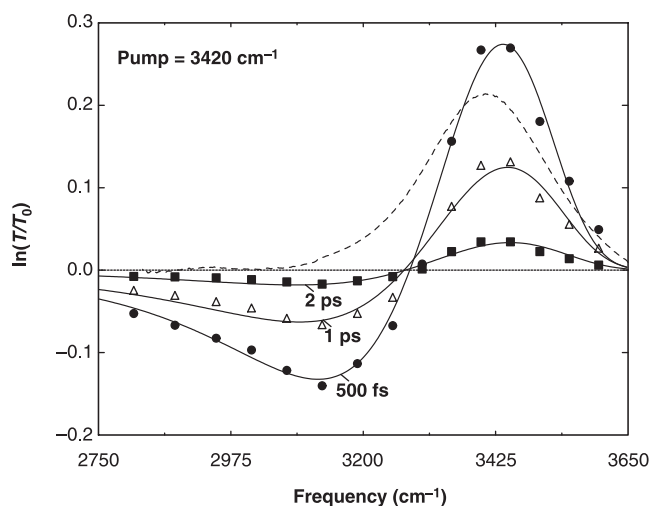


Fig. 2. Pump-probe transients of 0.5 M HDO dissolved in liquid D₂O measured at four different probe frequencies. The solid curves are calculated with the quantum-mechanical LS model.

stretch vibration. We use an adiabatic approach, which implies that the Schrödinger equation is solved in r with R as a parameter. The solution is obtained numerically with the Numerov method (17). The resulting eigenenergies $E_v(R)$ are added to the potential-energy term $V_{II}(R)$ to form potential-energy functions $W_v(R)$ for each vibrational level v . The thermal distribution in $W_0(R)$ at 300 K leads to a calculated linear absorption spectrum with a width of 254 cm^{-1} that is nearly Gaussian in shape, but that is somewhat steeper on the high-frequency side than on the low-frequency side (Fig. 1), in good agreement with the experimental absorption spectrum. The energy difference $E_1(R) - E_0(R)$ corresponds to the fundamental O-H stretch frequency. The dependence of $E_1 - E_0$ on R is in excellent agreement with experimental observations (18, 19).

The functions $W_v(R)$ were used to calculate the transient spectra of Fig. 1 and the pump-probe transients of Fig. 2 (20). In this calculation, we took into account that the pump pulse excites only a subset of the thermal distribution in R . To account for the effects of homogeneous broadening, the pump-pulse spectrum was convolved with a Lorentzian with a width of 90 cm^{-1} (21). The excited subset evolves to the thermal distribution because R is subject to the spontaneous fluctuations of the liquid (9–11). These fluctuations were modeled with a diffusion equation in the hydrogen bond potentials $W_v(R)$ (22).

Figure 3 shows the potential $V_I(r,R)$ ob-

tained from fitting the transient spectra of Fig. 1. For $R \leq 2.7 \times 10^{-10}\text{ m}$, $V_I(r,R)$ becomes very broad in the energy region that corresponds to the $v = 2$ state. As a result, the $v = 2$ vibrational state becomes delocalized, which means that the hydrogen atom can be found both at a distance r_{OH} (the equilibrium O-H bond length in the $v = 0$ state) from the left oxygen of the O-H...O system and at a distance r_{OH} from the right oxygen atom. The delocalization of the hydrogen atom in the $v = 2$ state leads to a strong decrease of the energy E_2 . Therefore, the large width and strong broadening of the $v = 1 \rightarrow 2$ absorption spectrum to lower frequencies can be explained by the distribution of R covering transitions both to localized, high-energy $v = 2$ states ($R \geq 2.7 \times 10^{-10}\text{ m}$) and to delocalized, low-energy $v = 2$ states ($R \leq 2.7 \times 10^{-10}\text{ m}$). The shape of the potential $V_I(r,R)$ and the character of the vibrational wave functions agree well with the results of ab initio calculations of an aqueous hydrogen-bonded O-H...O system (23). In this theoretical study, the $v = 2$ state became strongly delocalized between the two oxygen atoms for $R < 2.8 \times 10^{-10}\text{ m}$.

The positions $R_{\text{eq},v}$ of the minima of the hydrogen bond potential-energy curves $W_v(R)$ are $R_{\text{eq},0} = 2.85 \times 10^{-10}\text{ m}$, $R_{\text{eq},1} = 2.80 \times 10^{-10}\text{ m}$, and $R_{\text{eq},2} = 2.65 \times 10^{-10}\text{ m}$. The decrease in $R_{\text{eq},v}$ with increasing quantum number v implies that the hydrogen bond contracts upon vibrational excitation. This contraction leads to a more delocalized character of the vibrational wave functions and thus to a decrease of the transition fre-

quencies. Hence, the contraction induces a delayed rise of the absorption in the red wing of the transient absorption spectrum, as is indeed observed in Fig. 2 at a probe frequency of 2840 cm^{-1} .

Excitation from $v = 0$ to the $v = 2$ state leads to a strong increase in the probability of finding the hydrogen atom near the right oxygen atom of the D-O-H...OD₂ system formed by an HDO and a D₂O molecule. Car-Parrinello molecular dynamics simulations showed that such a transfer of a hydrogen atom to the right oxygen atom is associated with a charge transfer, so that a proton, and not a hydrogen atom, is transferred (24). The potentials V_I and V_{II} can be used to calculate the energy $E_{T,v}$ required for proton transfer in each of the quantum states of the O-H stretch vibration. The proton acquires an appreciable probability near the right oxygen atom in the O-H...O system when the energy of the occupied vibrational state of the O-H stretch vibration exceeds $V_I(r,R)$ at $r = R - r_{\text{OH}}$. Hence, proton transfer can be induced by either shortening the oxygen-oxygen distance R or by exciting the O-H stretch vibration to a strongly delocalized state. The energies $E_{T,v}$ are shown in Fig. 4. For the $v = 0$ and $v = 1$ states, proton transfer requires a strong shortening of the O-H...O hydrogen bond, which has a high associated energy cost. For the $v = 2$ state, no contraction of the O-H...O hydrogen bond is required because of the delocalized character of the proton in this state. The proton is also delocalized in the $v = 3$ and $v = 4$ states, but these states require a larger excitation energy than

Fig. 3. Potential $V_I(r,R) = D_{\text{Ia}}[1 - \exp(-n_{\text{Ia}}(r - r_0)^2/2r)] + D_{\text{Ib}}[1 - \exp(-n_{\text{Ib}}(R - r - r_0)^2/2(R - r_0))]$ of an O-H...O system formed by an HDO and a D₂O molecule, for three discrete values of R . The parameters of $V_I(r,R)$ follow from various experimental observations. The energy D_{Ia} equals the O-H binding energy of water of $38,750\text{ cm}^{-1}$ (4.8 eV); n_{Ia} is determined by the frequency of the O-H stretch vibration and equals $9.8 \times 10^{10}\text{ m}^{-1}$; r_0 equals the gas-phase O-H bond length of $0.97 \times 10^{-10}\text{ m}$; D_{Ib} follows from the relations between the O-H bond length, the O-H stretch vibrational frequency, and the oxygen-oxygen distance R . An excellent description of these relations is obtained with $D_{\text{Ia}}/D_{\text{Ib}} \approx 1.5$ (15). Here we use $D_{\text{Ib}} = 25,000\text{ cm}^{-1}$ (3.1 eV). The parameter n_{Ib} follows from a fit to the measurements of Figs. 1 and 2 and has a value of $16.5(1.0) \times 10^{10}\text{ m}^{-1}$. Also shown are the three lowest-energy ($v = 0, 1, 2$) vibrational wave functions in the potential for $R = 2.70 \times 10^{-10}\text{ m}$.

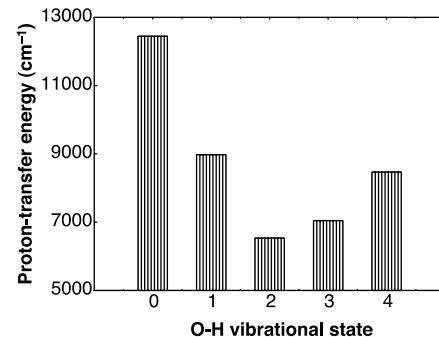
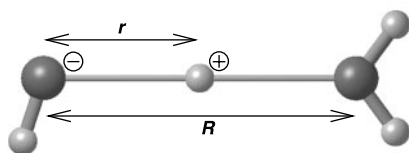
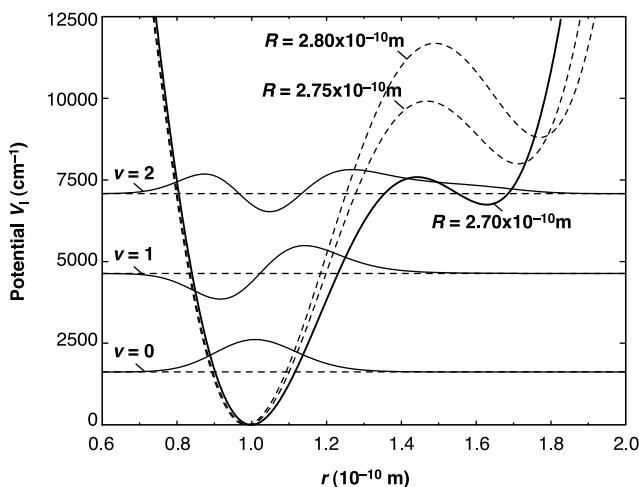


Fig. 4. Calculated energy $E_{T,v}$ required for proton transfer in an O-H...O system formed by an HDO and a D₂O molecule, for the five lowest quantum states v of the O-H stretch vibration. These energies are calculated by solving $E_v(R) = V_I(r = R - r_{\text{OH}}, R)$ for the oxygen-oxygen distance R . The value of R at which this equality holds is denoted as $R_{T,v}$. We find $R_{T,0} = 2.44 \times 10^{-10}\text{ m}$, $R_{T,1} = 2.50 \times 10^{-10}\text{ m}$, and $R_{T,2} = 2.60 \times 10^{-10}\text{ m}$. For the higher vibrational states ($v \geq 3$), $R_{T,v} > R_{\text{eq},v}$, which means that the energy $E_v(R)$ already exceeds $V_I(r = R - r_{\text{OH}}, R)$ at the equilibrium distance $R_{\text{eq},v}$. The proton-transfer energy $E_{T,v}$ is given by $E_{T,v} = E_v(R_{T,v}) + V_{II}(R_{T,v}) - E_0(R_{\text{eq},0}) - V_{II}(R_{\text{eq},0})$, with $R_{\text{eq},0} = 2.85 \times 10^{-10}\text{ m}$.

the $\nu = 2$ state. Hence, the $\nu = 2$ state has the lowest proton-transfer energy. The energy $E_{T,2}$ of 6500 cm^{-1} (0.82 eV) is less than 20% of the O-H binding energy of $38,750\text{ cm}^{-1}$ (4.8 eV), which shows that the hydrogen bonds in liquid water have a surprisingly strong effect on the properties of the O-H chemical bond.

For pure H_2O , the interactions between the O-H stretch vibrations and the O-H...O hydrogen bonds are quite similar to those in a solution of HDO in D_2O . Therefore, the same qualitative behavior is expected for the vibrational states of hydrogen-bonded H_2O molecules. However, quantitatively there will be small differences, because the O-H stretch vibrations of the H_2O molecule form delocalized symmetric and asymmetric modes.

The strongly delocalized nature of the excited vibrational states of the O-H stretch vibration can have important implications for the mechanism of proton transfer in room-temperature water. Recent Car-Parrinello molecular dynamics simulations showed that the first step of the autodissociation of water



is formed by the transfer of a proton in the O-H...O system (24). In view of this finding, it is interesting to compare the activation energy of the autodissociation of water with the proton-transfer energies shown in Fig. 4. A water molecule dissociates every 11 hours at 298 K ($k_D = 2.4 \times 10^{-5}\text{ s}^{-1}$) (25) and every 214 hours at 273 K ($k_D = 1.3 \times 10^{-6}\text{ s}^{-1}$) (26), from which the activation energy can be estimated to be $\sim 6600\text{ cm}^{-1}$. This activation energy is much lower than the energy of $12,500\text{ cm}^{-1}$ required for proton transfer in the vibrational ground state and quite similar to the energy of 6500 cm^{-1} of proton transfer through excitation of the $\nu = 2$ state. Hence, it seems likely that the first step of the autodissociation proceeds through an excited vibrational O-H stretch vibrational state, most probably $\nu = 2$. Unfortunately, this notion cannot be further experimentally tested by vibrationally exciting water and probing the reaction products, because the energy equilibration of water is too fast to determine the excited degree(s) of freedom through which the products were formed. However, the present findings on the delocalized character of the excited O-H stretch vibrational states should stimulate theoretical work on the reactivity of the O-H groups of water that explicitly includes the quantum-mechanical nature of the proton motion.

References and Notes

1. C. J. T. de Grotthuss, *Ann. Chim.* **58**, 54 (1806).
2. M. Tuckerman, K. Laasonen, M. Sprik, M. Parrinello, *J. Chem. Phys.* **103**, 150 (1995).
3. ———, *J. Phys. Chem.* **99**, 5749 (1995).
4. D. Marx, M. Tuckerman, J. Hutter, M. Parrinello, *Nature* **397**, 601 (1999).
5. A. Lock, S. Woutersen, H. J. Bakker, *J. Phys. Chem. A* **105**, 1238 (2001).

6. S. Woutersen, U. Emmerichs, H.-K. Nienhuys, H. J. Bakker, *Phys. Rev. Lett.* **81**, 1106 (1998).
7. J. Deak, S. Rhea, L. Iwaki, D. Dlott, *J. Phys. Chem. A* **104**, 4866 (2000).
8. S. Woutersen, U. Emmerichs, H. J. Bakker, *Science* **278**, 658 (1997).
9. R. Laenen, C. Rauscher, A. Laubereau, *Phys. Rev. Lett.* **80**, 2622 (1998).
10. G. M. Gale, G. Gallot, F. Hache, N. Lascoux, S. Bratos, J.-C. Leicknam, *Phys. Rev. Lett.* **82**, 1086 (1999).
11. S. Woutersen, H. J. Bakker, *Phys. Rev. Lett.* **83**, 2077 (1999).
12. ———, *Nature* **402**, 507 (1999).
13. Independently tunable mid-IR pump and probe pulses are generated through parametric amplification processes in β -barium borate (BBO) and potassium titanyl phosphate (KTP) crystals that are pumped by the pulses (800 nm, 100 fs, 3 mJ, 1 kHz) delivered by a Ti:sapphire regenerative amplifier. The generated mid-IR pulses are tunable between 2.7 and $4\text{ }\mu\text{m}$ (2500 to 3700 cm^{-1}); they have a pulse duration of 200 fs and an energy per pulse of $20\text{ }\mu\text{J}$ (pump) and $2\text{ }\mu\text{J}$ (probe). The pump and probe pulses are focused to a common focal spot with a diameter of $\sim 100\text{ }\mu\text{m}$ in the sample.
14. H. Graener, G. Seifert, *J. Chem. Phys.* **98**, 36 (1993).
15. E. R. Lippincott, R. Schroeder, *J. Chem. Phys.* **23**, 1099 (1955).
16. F. Franks, Ed., *Water, a Comprehensive Treatise* (Plenum, New York, 1972).
17. G. Dahlquist, A. Björck, N. Anderson, *Numerical Methods* (Prentice-Hall, Englewood Cliffs, NJ, 1974).
18. A. Novak, *Struct. Bonding (Berlin)* **18**, 177 (1974).
19. W. Mikenda, *J. Mol. Struct.* **147**, 1 (1986).
20. The transient spectrum at a particular delay was

calculated by multiplying the time-dependent excited distributions in the potentials $W_0(R)$ and $W_1(R)$ with the R -dependent transition probabilities of the $\nu = 0 \rightarrow 1$ and $\nu = 1 \rightarrow 2$ transitions. These distributions were then translated into frequency-dependent functions by using the relations between R and the transition frequencies $[W_1(R) - W_0(R)]/h$ and $[W_2(R) - W_1(R)]/h$. To obtain the final calculated transient spectrum, the $\nu = 0 \rightarrow 1$ bleaching, the $\nu = 1 \rightarrow 0$ stimulated emission, and the $\nu = 1 \rightarrow 2$ induced absorption contributions were added and convolved with the probe spectrum and the homogeneous broadening.

21. J. Stenger, D. Madsen, P. Hamm, E. T. J. Nibbering, T. Elsaesser, *Phys. Rev. Lett.* **87**, 027401 (2001).
22. R. Kubo, M. Toda, N. Hashitsume, *Statistical Physics II, Nonequilibrium Statistical Mechanics* (Springer, Berlin, 1995).
23. W. A. P. Luck, T. Wess, *Can. J. Chem.* **69**, 1819 (1991).
24. P. L. Geissler, C. Dellago, D. Chandler, J. Hutter, M. Parrinello, *Science* **291**, 2121 (2001).
25. P. W. Atkins, *Physical Chemistry* (Oxford Univ. Press, Oxford, ed. 6, 1998).
26. W. C. Natzle, C. B. Moore, *J. Phys. Chem.* **89**, 2605 (1985).
27. We thank D. Frenkel for useful discussions. The research presented in this paper is part of the research program of the Stichting Fundamenteel Onderzoek der Materie (Foundation for Fundamental Research on Matter) and was made possible by financial support from the Nederlandse Organisatie voor Wetenschappelijk Onderzoek (Netherlands Organization for the Advancement of Research).

25 April 2002; accepted 31 May 2002

Selection and Amplification of Hosts From Dynamic Combinatorial Libraries of Macrocyclic Disulfides

Sijbren Otto,* Ricardo L. E. Furlan,† Jeremy K. M. Sanders

We have discovered two receptors for two different guests from a single dynamic combinatorial library. Each of the two guests amplifies the formation of a tightly binding host at the expense of unfit library members. Small differences in host-guest binding translate into useful differences in amplification. The selected hosts could be readily synthesized using biased dynamic libraries that contain only the right ratio of those building blocks that were selected by the guests. These results establish dynamic combinatorial chemistry as a practical method not only for the discovery but also for the synthesis of new receptors.

Molecular recognition leading to the binding of a guest to a host involves a complex interplay of subtle noncovalent interactions. The understanding of these interactions is limited, hampering successful design of new host-guest systems. Combinatorial methods in which a guest can choose from a pool of receptors can be useful tools to optimize designs, facilitate access to new hosts, and ul-

timately aid in the understanding of host-guest interactions. Dynamic combinatorial chemistry (1–3) goes a step further: the preferred receptor is not only selected by the guest but also amplified at the expense of the unselected compounds. The key feature of dynamic combinatorial chemistry is the reversible nature of the reaction that links building blocks together (4) to form a mixture of compounds [a dynamic combinatorial library (DCL)] that interconvert continuously (Fig. 1). The composition of a DCL is under thermodynamic control, that is, the concentration of each library member is determined by its free energy. Molecular recognition events that lead to the stabilization of a particular member of the library induce a shift of

Department of Chemistry, University of Cambridge, Lensfield Road, Cambridge CB2 1EW, UK.

*To whom correspondence should be addressed. E-mail: so230@cam.ac.uk

†Present address: Universidad Nacional de Rosario, Facultad de Ciencias Bioquímicas y Farmacéuticas, Suipacha 531, 2000 Rosario, Argentina.